

Palladium Clusters Anchored on Graphene Vacancies, and their Effect on the Reversible Adsorption of Hydrogen.

María J. López,* Iván Cabria, and Julio A. Alonso

Departamento de Física Teórica, Atómica y Óptica, University of Valladolid, 47011

Valladolid, Spain

Phone: +34 983 184436

E-mail: maria.lopez@fta.uva.es

*To whom correspondence should be addressed

Abstract

The hydrogen storage capacity of nanoporous carbons can be enhanced through metal doping, for instance doping with palladium. However, there are two problems that may limit the positive effect of metal doping on the reversible storage capacity. First, clustering of the metal atoms decreases its effectiveness, which is largest for maximum dispersion. A second problem that is often overlooked, is that the desorption of metal-hydrogen complexes may compete favorably with the desorption of hydrogen molecules. Desorption of complexes would spoil the reversible storage of hydrogen in the material. Both problems can be avoided by firmly anchoring the metal atoms and clusters to defects of the carbon substrate, for instance vacancies. With this goal in mind, we have performed Density Functional calculations to investigate the desorption of hydrogen and of Pd-hydrogen complexes from Pd atoms and clusters supported on pristine graphene and on graphene layers with vacancies. We show that palladium atoms bind much stronger to graphene vacancies, binding energy $E_b = 5.13$ eV, than to pristine graphene, $E_b = 1.09$ eV. The Pd atoms tend to nucleate and form clusters around the vacancies and the small Pd_n clusters ($n = 2 - 6$) also bind strongly, $E_b \sim 5$ eV, to the vacancies. However, the Pd-Pd interaction is much smaller than the Pd-vacancy interaction and, therefore, the vacancies favor the dispersion of palladium on the graphene layer. For hydrogen adsorbed on Pd atoms and clusters supported on pristine graphene, desorption of Pd-hydrogen complexes competes with desorption of molecular hydrogen. However, for hydrogen adsorbed on a Pd atom anchored on a graphene vacancy, the desorption of the PdH_2 complex costs 4.2 eV and, therefore, it does not compete with the desorption of molecular hydrogen, which takes place with an energy cost of only 0.2 eV. This shows the beneficial effect that anchoring Pd atoms and clusters to graphene vacancies has on the reversible adsorption/desorption of hydrogen.

Keywords: Hydrogen Storage, Nanoporous Carbons, Metal Doping, Simulation, DFT

Introduction

Many efforts are now dedicated to find clean fuels that could replace gasoline in transportation vehicles, and hydrogen is considered to be a firm candidate.¹ The basis of this application is the reaction of hydrogen with atmospheric oxygen in a hydrogen fuel cell, producing an electric current. The only emission from the reaction is water. However, hydrogen is a gas, and the bottleneck of this technology, as it is pointed out in a recent review by Jena,² is to find an efficient way to store hydrogen in a tank, to be able to run the car for about 600 Km. A promising method is the storage of hydrogen in light solid porous materials, and the mechanism of storage is the adsorption of H₂ on the inner walls of the pores. Porous materials show large specific surface areas of several thousand m²/g. A particular class of those materials is nanoporous carbon.³ Thermodynamic estimations by Li et al.⁴ indicate that the values of the adsorption energies that would lead to an efficient adsorption/desorption cyclic process at room temperature and moderate pressures are in the range of 0.3-0.4 eV per hydrogen molecule. This is a narrow window, intermediate between typical physisorption and chemisorption energies. The short-term targets proposed by the U.S. Department of Energy (DOE), which would permit using hydrogen as a fuel in onboard applications, are: a gravimetric storage capacity of at least 5.5% of hydrogen in weight, and a volumetric capacity of more than 0.040 Kg of hydrogen per liter at room temperature and moderate pressures.⁵ Experiments and calculations indicate that none of the current hydrogen storage methods and none of the known solid porous materials meet the DOE targets.^{3,6} In the case of porous carbons, the walls of the pores are similar to imperfect graphene layers,⁷ and the problem is that the adsorption energy of H₂ on graphene is low, below 0.1 eV/molecule.

Doping the carbon materials with metallic impurities is viewed as a promising strategy to enhance the hydrogen uptake.⁸⁻¹⁰ The metallic atoms have the effect of increasing the binding energies of molecular hydrogen to the pore walls.^{11,12} In addition, the deposited metallic atoms can bind several hydrogen molecules.¹³⁻¹⁶ The binding of molecular hydrogen to transition metals has been explained using the Kubas model¹⁷ as a donation of electronic

charge to the unfilled d-orbital of Pd followed by back donation from the transition metal to the antibonding orbital of H₂. On the other hand, a different mechanism, the polarization of the H₂ molecule, has been used to explain the binding of molecular hydrogen to metallic cations.¹⁸ An increase of the hydrogen storage capacities of carbon nanotubes doped with lithium and potassium has been observed,^{8,9} and the atypical hydrogen uptake observed by Bath et al.¹⁰ on chemically activated microporous carbon has been proposed to be due to traces of alkali metals residual from the process of chemical activation.

However, there are some difficulties with the doping of porous carbons. The first one is that aggregation of the adsorbed dopant atoms may occur, because the metal atom-metal atom bonding is usually stronger than the metal atom-graphene bonding.¹⁹⁻²¹ The effect of the metal dopant in enhancing the amount of hydrogen adsorbed would be largest for maximum dispersion of the dopant, that is, when metal atoms or very small clusters are present. Consequently, formation of large clusters should be avoided if possible. A second problem, usually unnoticed and that we point out in this work, may occur in the step of desorption of the adsorbed hydrogen, a key step to feed the hydrogen fuel cells. We show, for the case of Pd doping, that desorption of metal-hydrogen complexes often competes with desorption of H₂. Both problems are avoided by increasing the binding energy of the metal atoms or small metal clusters to the supporting carbon substrate. This can be achieved by anchoring the metal atoms and small clusters to defects in the carbon networks of the pore walls. It has been found that defects in graphene (such as mono- and di-vacancies) increase the adsorption energy of metal atoms and small metal clusters significantly, to the point of exceeding the cohesive energy of the metal.²²⁻²⁴ For this reason we investigate the anchoring of Pd atoms and small Pd clusters to monovacancies in graphene. The result is that the binding energy of Pd atoms and clusters to defects on the carbon substrate rises up to about 5 eV, whereas the adsorption energy on a carbon substrate with no defects is below 1.5 eV.

Theoretical Model

Computer simulations of the structure of nanoporous carbons indicate that the walls of the pores are planar or curved graphene-like layers containing defects.⁷ This means that in theoretical studies of the storage of hydrogen on the pores, the walls can be conveniently modeled as graphene walls. We have performed Density Functional (DFT) calculations to study i) the adsorption of H₂ on Pd atoms and small Pd clusters supported on graphene, ii) the adsorption of Pd atoms and small Pd clusters on a graphene monovacancy, and iii) the effect that anchoring the Pd atoms to graphene vacancies has on the adsorption-desorption of hydrogen. The DFT calculations have been performed using the supercell method, with a basis set of plane waves, and ultrasoft pseudopotentials,²⁵ as implemented in the DACAPO code.²⁶ The pseudopotential for Pd uses a Kr-like core. An energy cutoff of 350 eV was taken for the plane wave expansion of the wave functions, and a cutoff of 1000 eV for the electron density. Electronic exchange and correlation effects are treated by the generalized gradient approximation of Perdew and Wang²⁷ (PW91). Spin-polarized calculations have been performed in all cases. The supporting graphene layer was simulated as a periodically repeated unit cell consisting of 50 carbon atoms in the (x, y) plane. The cell parameter in the direction perpendicular to the graphene plane was 14 Å. The selected supercell size is sufficiently large as to minimize the interaction between defects and clusters in different cells. The Monkhorst-Pack²⁸ k-point set of [2, 2, 1] in the reciprocal lattice is sufficient to guarantee convergence in the cohesive and adsorption energies within 10 meV. For Pd_n ($n = 1 - 5$) on pristine graphene, with and without hydrogen adsorbed, the selected values of the number of atoms per cell, the cell parameter in the direction perpendicular to the graphene layer, and the k-point set were 32, 12 Å, and [4, 4, 1], respectively. All the structures of isolated Pd_n, Pd_n on graphene and on a graphene monovacancy, and of molecular and dissociated hydrogen adsorbed on those Pd clusters have been optimized using a local minimization procedure based on molecular dynamics, until the forces on all atoms were smaller than 0.05 eV/Å. The search for global minima has been performed, based on our previous experience

in these systems, by considering a sufficiently large number of different guessed structures as the initial configurations to be optimized.

Desorption of adsorbed hydrogen and competition of metal-hydrogen complexes

A study of free Pd_n clusters ($1 \leq n \leq 6$) and Pd_n clusters supported on the surface of pristine graphene has been reported in previous papers.^{19,29} A salient feature is that Pd atoms have a strong tendency to form three dimensional structures, both as free clusters and also when supported on graphene. The binding energy of a Pd atom or a Pd_n cluster to pristine graphene is given by

$$E_b(\text{Pd}_n \text{ on G}) = E(\text{G}) + E(\text{Pd}_n) - E(\text{Pd}_n \text{ on G}) , \quad (1)$$

where $n = 1$ for the case of a Pd atom, G represents the supporting graphene layer (latter in the paper G will represent the graphene layer with a vacancy), and E indicates total energies. Then, the calculated binding energy of a Pd atom is $E_b(\text{Pd}) = 1.09$ eV. The binding energies of small Pd clusters are also moderately low, ranging from 0.49 to 1.26 eV for $n = 2-6$. These are also the energies required to desorb the Pd atoms and clusters from the graphene surface, as reported in Table 1. As a second step, we have also investigated the adsorption of hydrogen on the supported palladium atoms and clusters.²⁹ The adsorption of H_2 on the supported Pd clusters produces two types of adsorption states. The first one is an activated state of the adsorbed hydrogen molecule, with the H-H distance stretched and the bond weakened, although not broken. This type of adsorption occurs with no barriers, and the binding energies fit in a range of values of interest for achieving reversible hydrogen storage. The second type is characterized by dissociation of the hydrogen molecule and chemisorption of the two hydrogen atoms. Supported single Pd atoms are not able to dissociate the hydrogen

Table 1: Energy required for desorption of the cluster Pd_n ($n = 1 - 6$) from the Pd_n -graphene system. Also, energy required for desorption of the H_2 molecule and the Pd_nH_2 complex, respectively, from the H_2 - Pd_n -graphene system in the case of hydrogen adsorbed in the activated molecular state. In the case of the 2H_2 -Pd-graphene system (second line of the table) the desorption of H_2 corresponds to desorption of the first hydrogen molecule, and the complex desorbed is $\text{Pd}(\text{H}_2)_2$. The last column is the loss of stability of the supported Pd_n due to the adsorption of hydrogen in the activated state. Energies are given in eV.

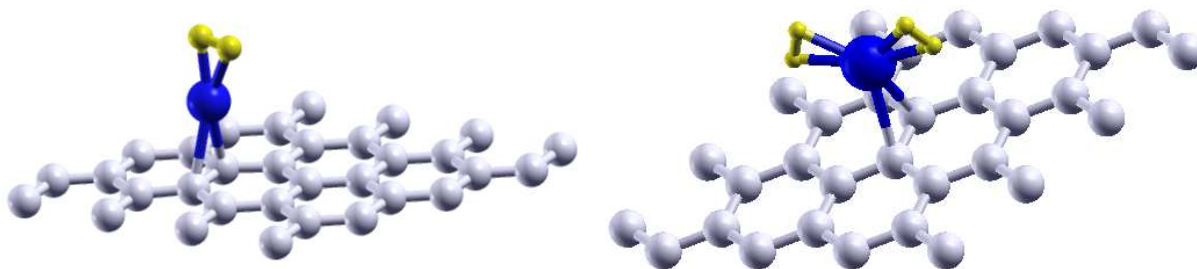
System	desorption of H_2	desorption* of Pd_nH_2	desorption* of Pd_n	loss of Pd_n stability
H_2 -Pd-graphene	0.96	0.93	1.09	0.16
2H_2 -Pd-graphene	0.25	0.25	1.09	0.84
H_2 - Pd_2 -graphene	1.06	0.97	1.26	0.29
H_2 - Pd_3 -graphene	0.53	0.77	0.76	-0.01
H_2 - Pd_4 -graphene	0.42	0.63	0.84	0.21
H_2 - Pd_5 -graphene (trigonal bipyramid)	0.69	0.60	0.49	-0.11
H_2 - Pd_6 -graphene	0.56	1.00	1.14	0.14

* desorption energies are calculated with respect to the free cluster or complex in the same isomeric configuration as the adsorbed one.

molecule; they adsorb H_2 in the activated state, exclusively. Beginning with supported Pd_2 , the two types of adsorption states are possible, the chemisorbed state of hydrogen being more stable. The dissociative chemisorption occurs with no barrier on supported Pd_2 and Pd_3 (starting from free gaseous H_2). But, in the case of Pd_4 and larger supported clusters there are barriers for the dissociative chemisorption of H_2 . The chemisorption binding energies are large, and it will be difficult to desorb the chemisorbed H atoms. Consequently, these are of less practical interest for hydrogen storage (see, however, some comments on the spillover mechanism in the final section of the paper).

In a recent work on the storage of hydrogen in porous carbon doped with palladium, Contescu et al.³⁰ reported that 18% of the palladium was in the form of adsorbed single atoms. The study of the interaction of H_2 with a Pd atom adsorbed on graphene is then a topic of high interest. Figure 1 shows the ground state structure for one and two H_2 molecules adsorbed on a Pd atom supported on a graphene layer. The Pd atom is in a bridge position above the bond between two adjacent carbon atoms. Adsorption of the H_2

Figure 1: Adsorption of one and two hydrogen molecules by a Pd atom supported on graphene. The bond length of the molecule is $d(\text{H-H}) = 0.86 \text{ \AA}$ and 0.85 \AA , respectively.



molecules on the supported Pd atom occurs without activation barrier, and the H–H bond length increases from its original value of 0.754 \AA in the free molecule to a value of 0.86 \AA or 0.85 \AA in the adsorbed state (for adsorption of one and two molecules, respectively), but the H–H bond is not broken. The adsorption energies of the hydrogen molecules on the

Pd_n -graphene system are given by

$$E_{ad}(mH_2) = E(Pd_n \text{ on G}) + m E(H_2) - E(mH_2 + Pd_n \text{ on G}) , \quad (2)$$

where the symbols E and G have the same meaning as in Eq. 1, m is the number of adsorbed molecules, and $E(mH_2 + Pd_n \text{ on G})$ is the energy of the system formed by the m hydrogen molecules adsorbed on Pd_n -graphene. When only one hydrogen molecule ($m=1$) is adsorbed, then $E_{ad}(H_2) = 0.96$ eV. This is also the energy $E_{de}(H_2)$ necessary to desorb the molecule in the step of releasing the stored hydrogen to be used as fuel. In comparison, the energy to desorb the PdH_2 complex

$$E_{de}(Pd_nH_2) = E(G) + E(Pd_nH_2) - E(H_2 + Pd_n \text{ on G}) , \quad (3)$$

is 0.93 eV for $n = 1$. This indicates that desorption of the PdH_2 complex will compete with desorption of the H_2 molecule, because the two desorption energies have nearly the same value. The difference $E_{loss} = E_b(Pd \text{ on G}) - E_{de}(PdH_2) = 0.16$ eV is the loss of stability of the supported Pd atom due to the adsorption of the hydrogen molecule. For adsorption of two molecules, the adsorption energy is $E_{ad}(2H_2) = 1.20$ eV. Desorption of the first H_2 molecule requires an amount of energy equal to 0.25 eV, and desorption of the second requires 0.96 eV. However, desorption of the whole complex $Pd(H_2)_2$ only costs 0.25 eV. Consequently, desorption of the $Pd(H_2)_2$ complex competes with desorption of the first hydrogen molecule, and it is more favorable than desorbing the two H_2 molecules. The loss of stability of the Pd atom due to the adsorption of two hydrogen molecules is substantial, $E_{loss} = 1.09 - 0.25 = 0.84$ eV. In conclusion, desorption of the PdH_2 or $Pd(H_2)_2$ complexes may limit the contribution of the Pd adatoms to the reversible hydrogen storage capacity of Pd-doped porous carbons.

Table 1 shows the desorption energies of H_2 adsorbed on Pd_n clusters supported on graphene, for the case of H_2 adsorbed in the activated state. These desorption energies are

equal to the corresponding adsorption energies given by Eq. 2. Also reported in the Table are the desorption energies (Eq. 3) of the Pd_nH_2 complexes adsorbed on graphene. Desorption of the Pd_nH_2 complexes competes with desorption of H_2 , since the two desorption energies are similar. In several cases, $n = 1, 2,$ and 5 , the desorption of the complex is slightly favored against desorption of hydrogen. For $n = 3$ and 4 , the desorption of complexes is also competitive, because it costs only 0.2 eV more than the desorption of H_2 . The first case when the competition is not significant corresponds to desorption from the largest supported Pd cluster studied, that is, Pd_6 . Desorption of H_2 is favored in that case because it requires 0.56 eV, whereas desorption of the Pd_6H_2 complex costs 1.0 eV. The overall result is that desorption of molecular hydrogen is inhibited, or at least reduced by the desorption of the Pd-H complexes for supported Pd atoms and Pd_n clusters for $n < 6$. The loss of stability of the adsorbed Pd cluster, defined as the difference between the desorption energy of Pd_n and the desorption energy of Pd_nH_2 , is given in the last column of the Table.

Desorption of molecular hydrogen from its dissociated (chemisorbed) state on Pd clusters supported on graphene is much costly. The hydrogen desorption energies (equal to the adsorption energies given by Eq. 2, where now $E(m\text{H}_2 + \text{Pd}_n \text{ on G})$ should be the energy of the system formed by m dissociated hydrogen molecules chemisorbed on Pd_n -graphene) are about two to four times higher than the corresponding desorption energies for the case of H_2 adsorbed in the activated state (compare Table 2 and Table 1) and much larger than the energies to desorb the Pd_nH_2 complexes with dissociated hydrogen (given by Eq. 3, and reported in Table 2). Therefore, desorption of the complexes with dissociated hydrogen is favored against desorption of hydrogen from the chemisorbed state, the only exception occurring for the largest cluster considered, Pd_6 . As an example, desorption of H_2 from Pd_2 requires an energy of 1.66 eV, and desorption of the Pd_2H_2 complex requires a smaller energy, 0.71 eV. Although the case of dissociated hydrogen chemisorbed on supported Pd clusters is of less practical interest because of the high desorption energies (larger than 1 eV), the overall conclusion is the same as for the case of adsorbed hydrogen in the activated

state: desorption of hydrogen-palladium complexes will inhibit the desorption of hydrogen. The competitive desorption energies of the Pd_2H_2 complexes arise from the relatively weak

Table 2: Energy required for desorption of H_2 and Pd_nH_2 , respectively, from the $\text{H}_2\text{-Pd}_n\text{-graphene}$ system in the case of dissociated hydrogen chemisorbed on the supported Pd cluster. The last column is the loss of stability of the supported Pd_n due to the chemisorption of hydrogen. Energies are given in eV.

System	desorption of H_2	desorption* of Pd_nH_2	loss of Pd_n stability
$\text{H}_2\text{-Pd}_2\text{-graphene}$	1.66	0.71	0.55
$\text{H}_2\text{-Pd}_3\text{-graphene}$	1.95	0.89	-0.13
$\text{H}_2\text{-Pd}_4\text{-graphene}$	1.47	0.96	-0.12
$\text{H}_2\text{-Pd}_5\text{-graphene}$ (square pyramid)	1.24	0.66	0.02
$\text{H}_2\text{-Pd}_6\text{-graphene}$	1.19	1.30	-0.16

* desorption energies are calculated with respect to the free complex in the same isomeric configuration as the adsorbed one.

bonding of the Pd clusters to the graphene surface, that is, the small desorption energies of the Pd clusters from graphene (see Table 1). Moreover, the supported Pd clusters may lose stability upon adsorption of hydrogen (E_{loss} given in Tables 1 and 2 is in many cases positive) in both cases of adsorption in the activated and the dissociated states.

There is another effect that inhibits (or at least reduces) the desorption of H_2 from the activated states. The heights of the energy barriers separating the activated adsorbed states of H_2 molecules and the dissociated (chemisorbed) states are 0.73, 0.26 and 0.31 eV on supported Pd_4 , Pd_5 and Pd_6 , respectively. These values are similar to the desorption energies of the activated H_2 molecules. This means that when heating the system in the step of releasing the stored hydrogen, many of the activated hydrogen molecules will reach the stable chemisorbed state, instead of being desorbed. Reaction times, τ , for the transition

from the activated to the dissociated state can be estimated from the equation

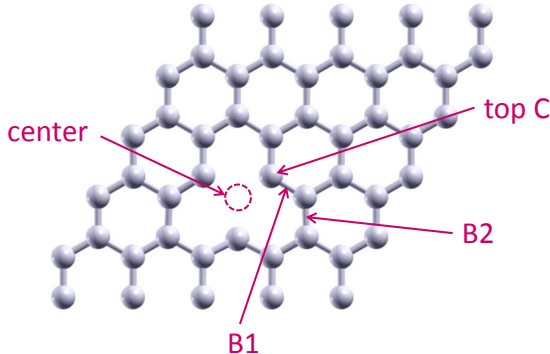
$$\tau = \frac{1}{\nu e^{\left(\frac{-E_b}{kT}\right)}}, \tag{4}$$

where ν is of the order of 10^{12} Hz, T is the temperature, and E_b is the activation barrier for dissociation of hydrogen from the activated state. At room temperature, the calculated reaction times are 1.81 s, 2.3×10^{-8} s, and 1.6×10^{-7} s on supported Pd₄, Pd₅ and Pd₆, respectively. This indicates that for Pd₄ the system will survive at the molecular state long enough to have a chance to desorb at room temperature. However, for Pd₅ and Pd₆ the barrier is lower and the dissociation kinetics is much faster, and therefore one would not expect desorption of hydrogen but dissociation. The desorption of hydrogen from the dissociated states would take place at higher temperatures, due to their higher desorption energies. This process is of less interest for the reversible storage of hydrogen under mild conditions. In summary, the two effects discussed, a) desorption of complexes, and b) formation of chemisorbed states, compete with the desorption of H₂, casting serious doubts on the usefulness of doping porous carbons with Pd.

Palladium clusters anchored on graphene vacancies

The relatively weak bonding of Pd to the graphene surface may be a drawback for the reversible adsorption of hydrogen since, as discussed in the previous Section, desorption of the palladium–hydrogen complexes competes with desorption of H₂. A way to cure this drawback is to anchor tightly the Pd clusters to the carbon surface. This can be achieved by attaching the Pd clusters to defects in the carbon surface, instead of supporting them on the pristine surface. With this goal in mind, we investigate the adsorption of Pd atoms and clusters on a graphene layer with defects, focusing on one type of defects, the single vacancies, which are produced when one carbon atom is removed from the graphene lattice (see Fig 2). The vacancy formation energy, that is, the energy required to remove a carbon

Figure 2: Structure of a graphene vacancy. The labels indicate different types of adsorption sites for the Pd atoms.

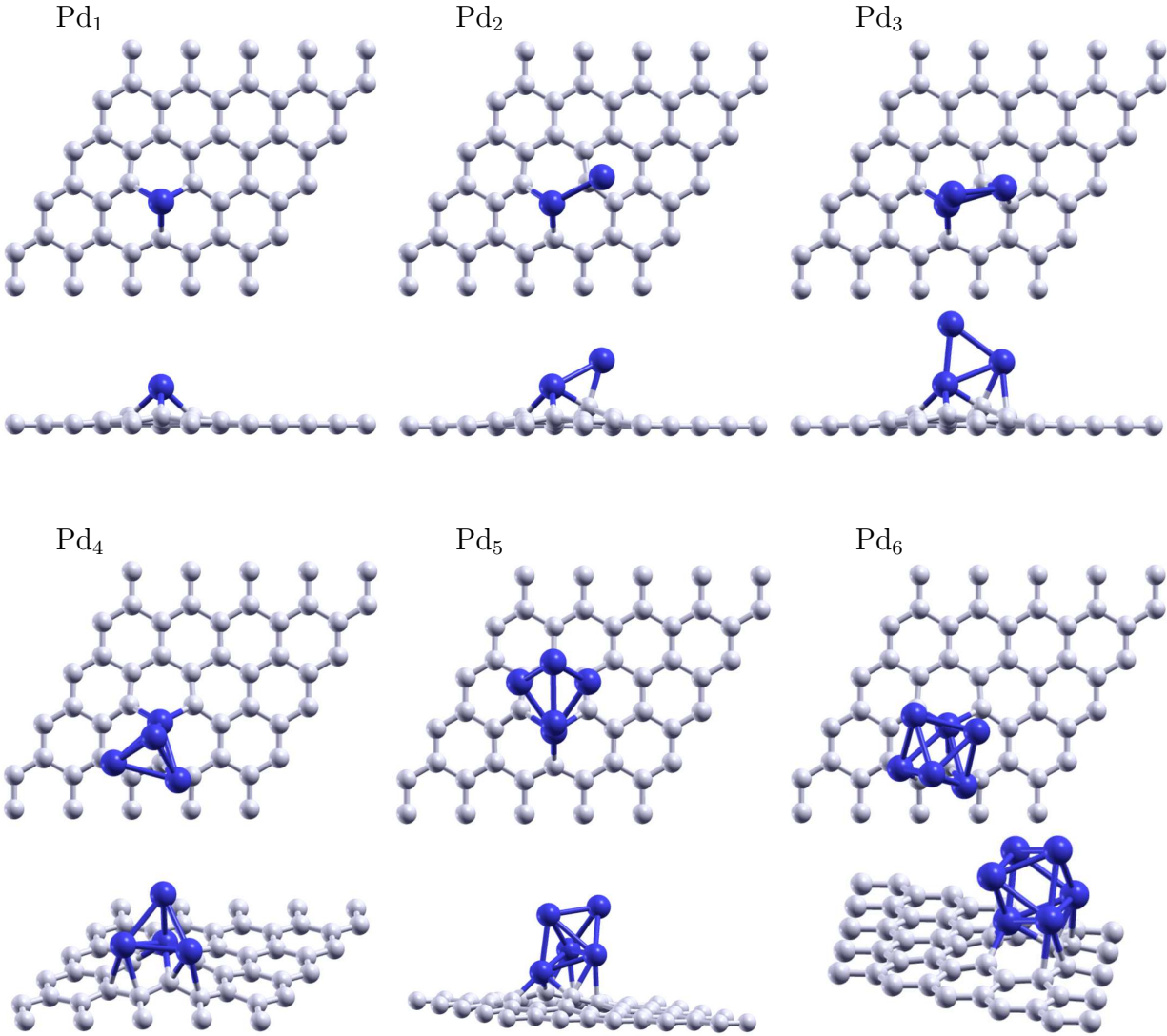


atom from a lattice site and putting the atom back at infinity in the lattice, is

$$E_{vac} = E(\text{graphene-vacancy}) - \frac{n-1}{n}E(\text{graphene}) , \quad (5)$$

where $E(\text{graphene})$ is the total energy of a supercell of pristine graphene containing n carbon atoms, and $E(\text{graphene-vacancy})$ is the energy of the same supercell of graphene in which one carbon atom has been removed. From DFT calculations we obtain $E_{vac} = 7.84$ eV, in good agreement with the experimental value³¹ of 7.0 ± 0.5 eV, and with other DFT calculations,^{23,32,33} which give values 7.7-7.8 eV. The optimized structure of the monovacancy has the three carbon atoms around the vacant site slightly displaced out of plane by 0.30, -0.14, and -0.11 Å, respectively. We have investigated the adsorption of Pd_n ($1 \leq n \leq 6$) clusters on a graphene vacancy. Figure 3 shows the optimized structures and Table 3 summarizes the binding energies and some structural data. A single palladium atom adsorbs on a graphene monovacancy above the vacant site at a distance of 1.56 Å from the graphene layer. The Pd atom is much larger than the C atoms and, therefore, Pd does not fit in-plane at the vacant site. The three C atoms around the vacancy move out of the graphene plane about 0.33 Å towards the Pd atom and the final distance between the Pd atom and the surrounding C atoms is 1.98 Å. The binding energy of Pd to a graphene vacancy is 5.13

Figure 3: Top and side views of the optimized structures of Pd_n clusters ($1 \leq n \leq 6$) adsorbed on a graphene vacancy.



eV (as calculated from eq. 1, where G now represents the graphene layer with a vacancy). This energy is much higher than the binding energy, 1.09 eV, of Pd to the pristine graphene surface. A Pd atom on pristine graphene sits above a C–C bond at a distance of 2.23 Å from the graphene layer. Clearly, Pd atoms deposited on graphene have a strong preference for the vacant sites in graphene. Figure 4 shows the electronic density redistribution, $\Delta\rho$, upon adsorption of a Pd atom on a) a graphene vacancy and b) pristine graphene. $\Delta\rho$ for

Table 3: Optimized structures of Pd_n clusters adsorbed on a graphene vacancy. $d_{\text{Pd-graphene}}$ are the distances of the Pd atoms to the graphene layer. E_b is the binding energy of the Pd_n cluster to the vacancy. $E_b^{\text{last-atom}}$ is the energy required to remove a single Pd atom from the Pd cluster adsorbed on the graphene vacancy. Distances are given in Å and energies are given in eV.

n	structure	$d_{\text{Pd-graphene}}$	E_b	$E_b^{\text{last-atom}}$
1	center vacancy	1.56	5.13	
2	center-top C	1.78, 2.79	5.93	2.10
3	vertical triangle (center-B1)	1.72, 2.67 4.26	5.72	2.24
4	tetrahedron on face (center-B1-B2)	1.75, 2.55 2.65, 4.36	5.44	2.65
5	trigonal bipyramid on face (center-B1-B1)	1.77, 2.64 4.43, 4.74	5.54	2.47
6	octahedron on face (center-B1-B2)	1.77, 2.58 4.10, 4.89	5.62	2.77

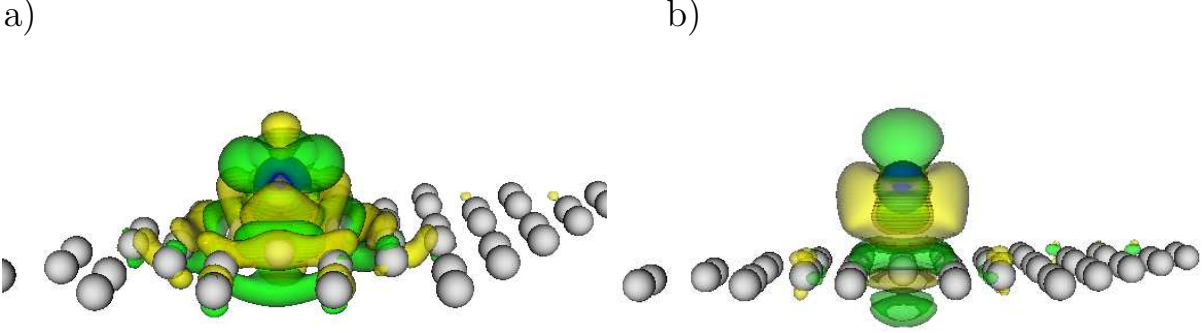
adsorption of a Pd atom or a Pd_n cluster is defined as

$$\Delta\rho = \rho(\text{Pd}_n \text{ on G}) - \rho(\text{Pd}_n) - \rho(\text{G}), \quad (6)$$

where $n = 1$ for the Pd atom, ρ is the electronic density, and G stands for either the graphene layer with a vacancy or the pristine layer. The redistribution of electronic density is larger in the case of the Pd adsorption on a vacancy, and it is accompanied by a charge transfer of $0.4 e$ from the Pd atom to the defective graphene layer. In contrast, there is a small charge transfer of $0.16 e$ from the Pd atom to the pristine layer, together with some polarization of the electronic density around the Pd atom. This reflects the stronger interaction of Pd with a graphene vacancy than with the pristine layer.

A second Pd atom adsorbs next to the first one, on top of one of the C atoms around the vacancy (see Fig. 3). The second Pd binds directly to both, the Pd atom saturating the vacancy and the graphene layer. The binding energy of the second Pd atom to the

Figure 4: a) Electronic density difference, $\Delta\rho$, between the system formed by a Pd atom adsorbed on a graphene vacancy and the two separated subsystems, Pd atom and defective graphene. b) $\Delta\rho$ for Pd adsorbed on pristine graphene. Contour values ± 0.005 e/au³, yellow positive, green negative.



Pd-saturated vacancy is given by

$$E_b^{\text{last-atom}}(\text{Pd}) = E(\text{Pd}_{n-1} \text{ on G}) + E(\text{Pd}) - E(\text{Pd}_n \text{ on G}) , \quad (7)$$

where the symbol G here represents the supporting graphene layer with a vacancy. In the case under discussion, $n=2$, but eq. (7) applies also to the binding energy of the last Pd atom of larger supported Pd clusters. This energy can be interpreted as the evaporation energy of a Pd atom from the adsorbed Pd cluster. For $n = 2$, $E_b^{\text{last-atom}} = 2.10$ eV. This energy is higher than both, i) the evaporation energy, 1.47 eV, of a Pd atom from Pd₂ adsorbed on pristine graphene,¹⁹ and ii) the binding energy, 1.09 eV, of a single Pd atom to pristine graphene. The Pd₂ cluster binds to the graphene vacancy with a binding energy (eq. 1) of 5.93 eV. The interaction of Pd with the vacancy is much stronger than the Pd–Pd interaction (the binding energy of a free Pd dimer is 1.30 eV). Several low lying configurations of Pd₂ adsorbed on a vacancy are summarized in Table 4. All the structures have in common that one Pd atom sits above the center of the vacant site. The second Pd atom is attached to the first one, and binds directly to the graphene layer in the two configurations center-B1 and center-B2; however, the second Pd atom does not bind directly to graphene in the vertical

configuration in which the Pd dimer is perpendicular to the graphene layer.

Table 4: Low lying configurations of Pd_n clusters adsorbed on a graphene vacancy. The energies, ΔE , are given with respect to the ground state configurations of Table 3. Energies are given in eV.

n	structure	ΔE
2	center-B2	0.33
2	center-B1	0.34
2	center (vertical)	0.76
3	horizontal triangle (center-B1-B2)	0.12
3	horizontal triangle (center-B1-B1)	0.17
3	inverted vertical triangle (center)	0.62
4	tetrahedron on face (center-B1-B1)	0.03
4	tetrahedron on edge (center-B1)	0.14
5	trigonal bipyramid on face (center-B1-B2)	0.04
5	trigonal bipyramid on edge (center-B1)	0.06
5	square pyramid on triangular face (center-top-B1)	0.17
6	octahedron on face (center-B1-B1)	0.001
6	octahedron on edge (center-B1)	0.28
6	capped square pyramid on triangular face (center-top-B2)	0.38

Pd₃ forms a triangle oriented perpendicular to the graphene layer. The Pd atoms of the base of the triangle sit above the center of the vacancy and above a C-C bond (B1), respectively (see Fig. 3). The binding energy of Pd₃ to the graphene vacancy is 5.72 eV. Pd clusters attach strongly to vacancies in graphene, but the interaction with the vacancy does not affect much the Pd-Pd interaction: the energy to remove a Pd atom from a Pd₃ cluster adsorbed on a vacancy, 2.24 eV, is similar to the energy, 2.45 eV, to remove the atom from an isolated Pd₃ cluster. The energy difference between the perpendicular configuration and almost parallel configurations of Pd₃ in which all three Pd atoms attach directly to graphene is 0.12–0.17 eV (see Table 4). A similar energy difference,¹⁹ 0.19 eV, was found between perpendicular and parallel configurations of Pd₃ adsorbed on pristine graphene. The vertical inverted triangle configuration, is higher in energy, 0.62 eV above the lowest

energy configuration.

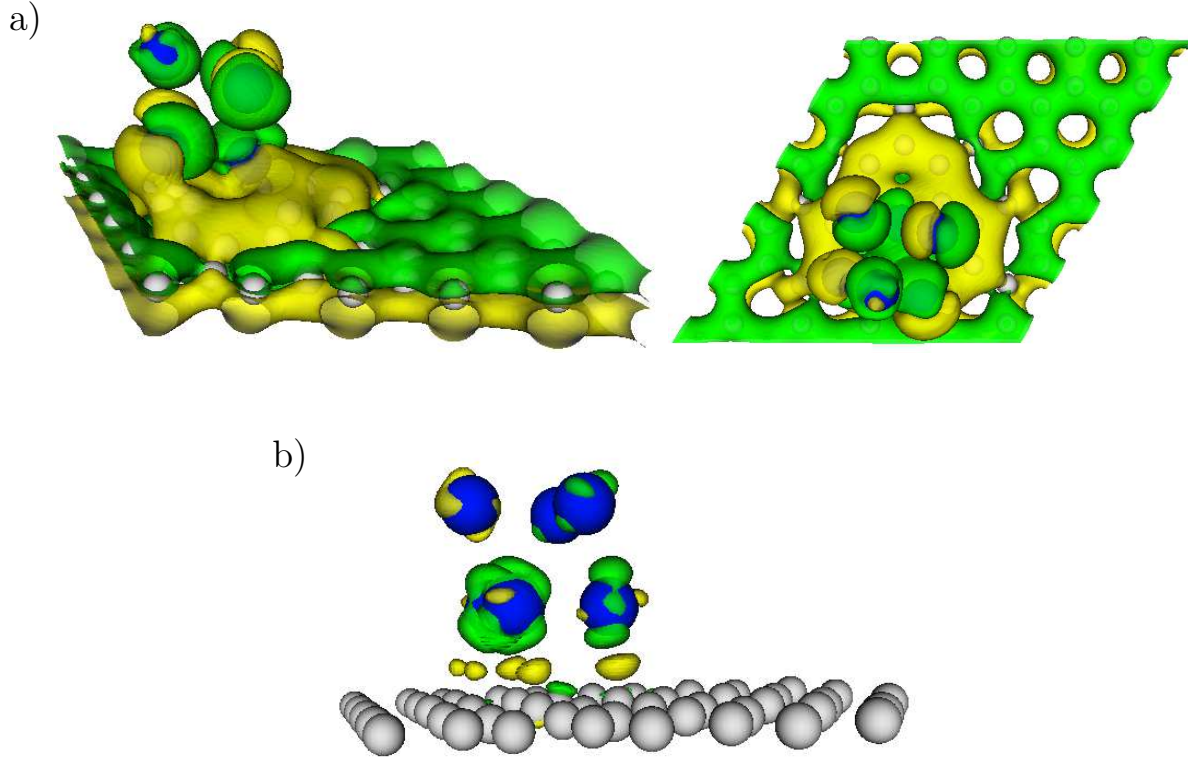
The lowest energy configuration of the Pd₄ cluster attached to a vacancy is the tetrahedral structure, the same as that of a free Pd₄ cluster. The tetrahedron rests on a triangular face with one Pd atom at the center of the vacancy. The binding energy of Pd₄ to the vacancy is 5.44 eV. This energy is substantially larger than the binding energy, 0.84 eV, of Pd₄ to pristine graphene. The energy required to remove one Pd atom from the cluster anchored on the vacancy is 2.65 eV. We have found other orientations of the Pd₄ tetrahedron anchored to the vacancy (see Table 4). The configurations with the tetrahedron laying on one face are almost degenerate. The configuration with the tetrahedron laying on one edge is 0.14 eV higher in energy. Planar configurations of the four Pd atoms are even higher in energy, 0.64 eV above the lowest energy configuration. This indicates that palladium does not wet the graphene surface. Instead, it prefers to form three-dimensional structures. Indeed, beginning with Pd₄, all the Pd_n clusters deposited on defective graphene have three-dimensional structures. The same behavior was found¹⁹ for Pd clusters deposited on pristine graphene.

There are two competing structures for the free Pd₅ cluster: the ground state trigonal bipyramid and the square pyramid, which is only 0.05 eV higher in energy. Upon deposition on pristine graphene, the square pyramid configuration becomes more stable by 0.14 eV, due to its stronger interaction with the graphene layer. Desorption of Pd₅ from the adsorbed square pyramid configuration (without changing its isomeric structure) costs 0.68 eV, whereas desorption from the adsorbed trigonal bipyramid configuration costs only 0.49 eV (see Table 1). However, adsorption on a vacancy preserves the energetic ordering of the isomers of the free cluster. The adsorbed square pyramid is 0.17 eV higher in energy (less stable) than the adsorbed trigonal bipyramid, which has a binding energy of 5.54 eV to the vacancy. The energy to remove one Pd atom from the anchored cluster is 2.47 eV. The trigonal bipyramid rests on a triangular face with the apex atom of one of the pyramids saturating the vacancy. Other orientations of the adsorbed trigonal bipyramid are almost degenerated in energy (see Table 4).

The lowest energy configuration of the isolated Pd_6 cluster is an octahedron. This structure is preserved, with minor distortion, upon adsorption on a graphene vacancy. The octahedron lies on a triangular face with one Pd atom saturating the vacancy. The binding energy of Pd_6 to the graphene vacancy is 5.62 eV. We notice from Table 3 that the binding energies of small Pd_n clusters ($n = 1 - 6$) to graphene vacancies are relatively high and do not depend much on cluster size, ranging from 5.13 to 5.93 eV. This reveals the localized nature of the interaction of the cluster with the vacancy. The cohesion inside the Pd cluster is not much affected by the adsorption at the vacancy. Thus, the energy of 2.77 eV necessary to remove one Pd atom from Pd_6 anchored on a vacancy is close to the evaporation energy, 2.69 eV, of a Pd atom from an isolated Pd_6 cluster. Therefore, for Pd clusters anchored on graphene vacancies, the evaporation of Pd atoms is favored over desorption of the entire cluster from the surface. In contrast, for Pd clusters adsorbed on pristine graphene, desorption of the entire cluster is preferred over evaporation of Pd atoms. Figure 5 shows the electronic density redistribution $\Delta\rho$, given by Eq. 6, upon adsorption of a Pd_6 cluster on a) a graphene vacancy and b) pristine graphene. Little redistribution of the electronic density occurs for adsorption on pristine graphene and, consequently, the binding energy of the Pd_6 cluster is quite low,²⁹ 1.14 eV. However, a substantial electron density redistribution takes place upon adsorption of Pd_6 on a graphene vacancy, consistent with its larger binding energy of 5.62 eV. Several low-lying configurations of Pd_6 adsorbed on a vacancy have been found. The two octahedral configurations sitting on one face are almost degenerated (see Table 4). The octahedral structure resting on one edge and the capped square pyramid resting on a triangular face are 0.28 and 0.38 eV higher in energy, respectively. Similarly as for smaller cluster sizes, a quasiplanar configuration of six Pd atoms (centered hexagon minus one atom) is quite high in energy, 1.67 eV above the lowest energy configuration, confirming the tendency of Pd to form three-dimensional structures.

The interaction of Pd with graphene vacancies is very strong. It doubles the strength of the Pd–Pd interaction, and is four times larger than the interaction of Pd with pristine

Figure 5: a) Side and top views of the electronic density difference, $\Delta\rho$, between a Pd₆ cluster adsorbed on a graphene vacancy and the two separated subsystems, Pd₆ cluster and defective graphene. b) $\Delta\rho$ for Pd₆ adsorbed on pristine graphene. Contour values ± 0.015 e/au³, yellow positive, green negative.



graphene. Therefore, Pd atoms dispersed on a graphene surface with defects will tend to saturate first all the vacancies, and then clusters will grow on the Pd-saturated vacancies. The vacancies favor the dispersion of Pd atoms on the surface of graphene and the Pd atoms and clusters get firmly anchored to vacancies. Clusters may also grow on the pristine surface of graphene. However, since the clusters bind weakly to the pristine surface, they will tend to migrate till they find a vacancy, a Pd-saturated vacancy, or other defects. In both cases, pristine graphene and graphene with vacancies, palladium does not wet the surface and exhibits a strong tendency to form three dimensional clusters.

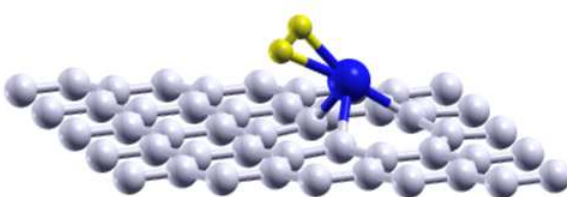
Although Pd atoms and bulk palladium metal are non-magnetic, the small Pd_{*n*} free clusters have a magnetic moment of $\mu = 2\mu_B$ for $2 \leq n \leq 6$. These moments are preserved upon deposition of the clusters on the surface of pristine graphene for $n = 3, 4$ and 6 , and

are quenched down to zero for $n = 2$ and 5. However, the adsorption of the Pd_n clusters on graphene vacancies leads to the quenching down to zero of all the magnetic moments, due to the stronger interaction of the Pd clusters with the defects.

Hydrogen adsorption/desorption from Pd atoms anchored on graphene vacancies

Above we have pointed out some problems associated to the desorption of molecular hydrogen adsorbed on Pd atoms and clusters supported on pristine graphene. Since some of those problems are rooted in the small binding between the Pd clusters and the carbon substrate, it is advisable to investigate the effect of anchoring the Pd clusters to vacancies in the carbon substrate. Our calculations show that the adsorption energy of molecular hydrogen on a Pd atom anchored on a graphene vacancy, calculated from Eq. 2 with $m = 1$ and $n = 1$, is 0.21 eV. Figure 6 shows the corresponding ground state structure. By looking at the desorption

Figure 6: Optimized structure of one hydrogen molecule adsorbed on a Pd atom anchored on a graphene vacancy. The bond length of the molecule is $d(\text{H-H}) = 0.79 \text{ \AA}$.

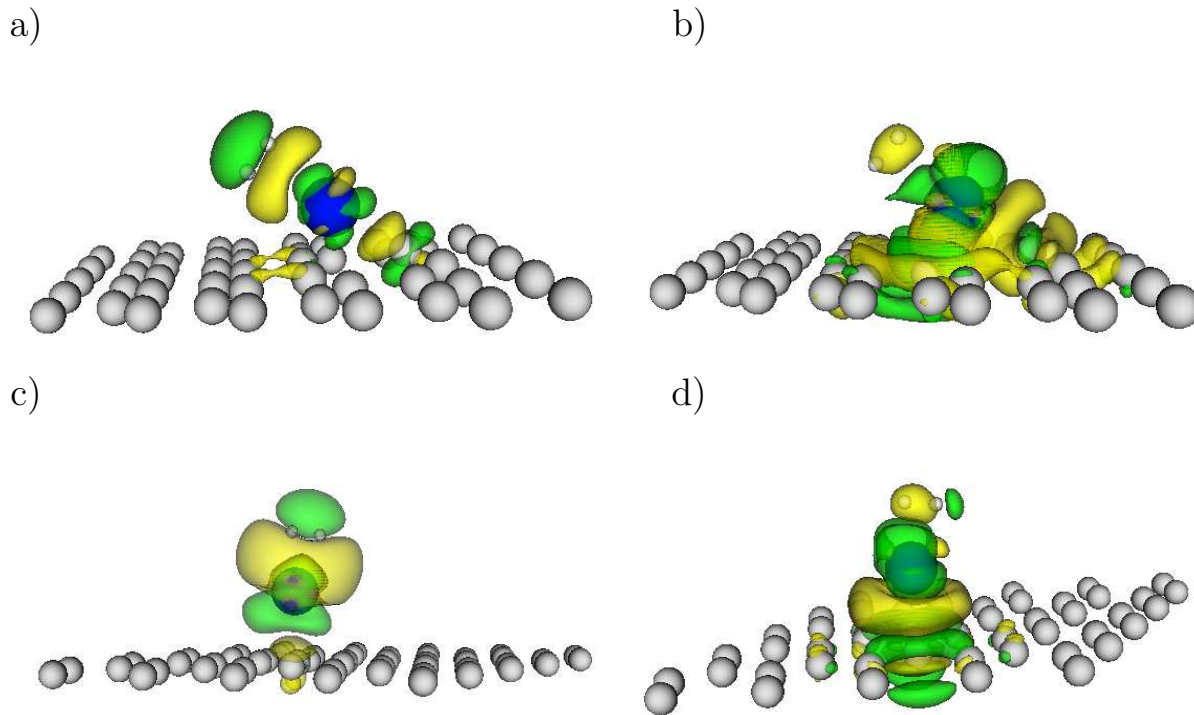


step, the energy required to desorb a hydrogen molecule from a Pd atom anchored at a graphene vacancy, is also 0.21 eV (equal to the adsorption energy). On the other hand, the desorption energy of the PdH_2 complex from the surface of the defective graphene is quite large, 4.22 eV, because the Pd atoms stay firmly anchored to the vacancies. Therefore, in contrast with Pd-doped pristine graphene, the desorption of the complex does not compete with the desorption of the hydrogen molecule. Figures 7 a) and c) show the electronic density

redistribution, $\Delta\rho$, upon adsorption of H_2 on a Pd atom anchored on a graphene vacancy and on a Pd atom adsorbed on pristine graphene, respectively. In both cases the hydrogen molecule becomes activated but the H–H bond is not broken. An accumulation of charge between the hydrogen molecule and the Pd atom is observed, responsible for the binding energy of the hydrogen molecule to the supported Pd atom. On the other hand, Figure 7 b) shows the electronic density difference, $\Delta\rho$, between the system formed by H_2 adsorbed on a Pd atom anchored on a graphene vacancy and the separated PdH_2 complex and graphene vacancy subsystems. The substantial $\Delta\rho$ reflects the bonding between the complex and the vacancy, which results in a large desorption energy of the complex. For comparison, Figure 7 d) shows the electronic density difference $\Delta\rho$ between the system formed by H_2 adsorbed on a Pd atom supported on pristine graphene and the separated PdH_2 complex and graphene layer subsystems. $\Delta\rho$ is in this case smaller, consistent with the smaller desorption energy of the complex from pristine graphene. In conclusion, anchoring the Pd atom tightly to the supporting layer solves the problem of the desorption of palladium–hydrogen complexes competing with the desorption of hydrogen.

The above result is promising in the attempt of achieving reversible adsorption-desorption of hydrogen. However, we notice a new difficulty: the adsorption energy of molecular hydrogen on the anchored Pd atom is 0.21 eV. This value is below the target value 0.3-0.4 eV established by Li et al.,⁴ although a different estimation by Bhatia and Myers³⁴ proposes a less conservative target value of 0.16 eV/molecule. The moderate adsorption energy of 0.21 eV contrasts with the substantial adsorption energies, 0.96 eV on Pd-doped pristine graphene, and 1.12 eV, of H_2 on a free Pd atom. In these three cases the hydrogen molecule becomes activated, with H–H bond distances of 0.79 Å, 0.86 Å, and 0.90 Å, respectively. The conclusion is that the magnitude of the adsorption energy of molecular hydrogen on Pd decreases, and the stretching of the H-H bond also decreases, as the strength of the interaction of the Pd atom with the supporting layer increases. That is, when the Pd atom exhausts a substantial part of its bonding capacity by interacting with the substrate, as is the case for

Figure 7: Electronic density difference, $\Delta\rho$, between H_2 adsorbed on Pd anchored on a graphene vacancy and: a) the two separated subsystems, H_2 molecule and Pd-saturated vacancy; b) the two separated subsystems, PdH_2 complex and the graphene vacancy. For comparison, we show the electronic density difference, $\Delta\rho$, between H_2 adsorbed on Pd-doped pristine graphene and: c) the two separated subsystems, H_2 molecule and Pd-doped pristine graphene; d) the two separated subsystems, PdH_2 complex and pristine graphene. Contour values $\pm 0.005 \text{ e/au}^3$, yellow positive, green negative. The blue sphere indicates the Pd atom, and the two small light spheres the hydrogen molecule.



Pd supported on the vacancy, the bonding with the H_2 molecule is weaker compared to the cases of free Pd or Pd on pristine graphene. This points to a general problem: it may be difficult to accomplish at the same time the two conditions of optimal H_2 adsorption energies (0.3-0.4 eV) and tightly anchored Pd clusters in the case of small Pd clusters (the situation for larger clusters may be different, and it is worth to be studied). As a way out of this problem we propose doping with nontransition metals. In a study of the effect of lithium doping¹¹ we noticed that the increase of the adsorption energy of H_2 to graphene arises from the electrical polarization of the molecule induced by the partially charged Li atom, and not from direct bonding with Li. This polarization effect does not decrease with the number of

hydrogen molecules around.

Summary and additional comments

The promising use of porous materials in hydrogen storage technologies is based on the reversible adsorption/desorption of hydrogen under mild pressure and temperature conditions. In this paper we have mainly focused on the desorption step of the cycle for Pd-doped nanoporous carbons. The pore walls have been modeled as pristine graphene layers and graphene layers with monovacancy defects. We have performed density functional calculations 1) of the decoration of pristine graphene and graphene vacancies with Pd atoms and clusters, and 2) of the adsorption of hydrogen on the supported Pd atoms and clusters. The binding energies of Pd atoms and small Pd clusters to pristine graphene are below 1.3 eV. The adsorption of hydrogen on Pd atoms and clusters supported on graphene occurs following two different adsorption modes: 1) adsorption of the molecule in an activated state, and 2) dissociation of the molecule and chemisorption of the two H atoms. The adsorption energies in the activated state lie in the range of interest for reversible storage of hydrogen. However, the desorption energy of the Pd_nH_2 complexes is smaller than or close to the desorption energy of the H_2 molecule for $n < 6$ and, therefore, desorption of the complexes competes with desorption of molecular hydrogen. Desorption of palladium–hydrogen complexes may then limit the contribution of the Pd adatoms and small clusters to the reversible hydrogen storage capacity of Pd–doped porous carbons. Starting with Pd_6 , the competition of complexes is not significant, and desorption of hydrogen is favored for both, the activated and the chemisorbed states. An additional difficulty that we have discussed is that heating the system during the desorption step may allow the activated molecular hydrogen to overcome the dissociation barrier and end up in the chemisorbed state.

Increasing the binding energy of the metal atoms and Pd clusters to the supporting carbon substrate would provide a way to overcome the problem of the competition from desorbing

Pd-H complexes. This can be achieved by anchoring the atoms and clusters to defects in graphene. Pd atoms and clusters attach firmly to graphene vacancies with binding energies of about 5 eV, in contrast with their weaker bonding, below 1.3 eV, to pristine graphene. We have investigated the adsorption of molecular hydrogen on Pd atoms anchored on graphene vacancies, and their corresponding desorption in competition with the desorption of the PdH₂ complex. Desorption of the PdH₂ complex costs 4.2 eV, in contrast with the small cost of 0.2 eV for desorption of H₂. Therefore, in this case desorption of the complex does not compete with desorption of hydrogen. Our study indicates that introducing defects on the carbon network of Pd-doped nanoporous carbons has two main beneficial effects: improving the dispersion of the metal on the carbon network, and preventing desorption of metal-hydrogen complexes, therefore enhancing the reversible adsorption-desorption of hydrogen in porous carbon materials. However, a problem still remains. In the process of desorption, the hydrogen molecule can follow a competing route, overcoming the dissociation barrier and ending up as a pair of chemisorbed H atoms.

In summary, the direct adsorption and desorption of hydrogen on the Pd clusters does not appear to be promising to enhance hydrogen storage in porous carbons doped with Pd. But, since the experimental evidence appears to indicate that hydrogen storage is enhanced by the presence of Pd clusters and nanoparticles, the only remaining possibility seems to be related with hydrogen spillover. Careful studies of this mechanism from the point of view of computational chemistry are recommended.

Acknowledgments

This work was supported by MICINN of Spain and the European Regional Development Fund (Grant MAT2011-22781) and by Junta de Castilla y León (Grant VA158A11-2).

References

- (1) Ogden, J. M. Hydrogen: The Fuel of the Future? *Phys. Today* **2002**, *55*(4), 69–75.
- (2) Jena, P. Materials for Hydrogen Storage: Past, Present, and Future. *J. Phys. Chem. Lett.* **2011**, *2*, 206–211.
- (3) Cabria, I.; López, M. J.; Alonso, J. A. In *Handbook of Nanophysics: Functional Materials Vol. 5*; Sattler, K., Ed.; CRC Press, Boca Raton, FL, 2010; pp 41.1–16.
- (4) Li, J.; Furuta, T.; Goto, H.; Ohashi, T.; Fujiwara, Y.; Yip, S. Theoretical Evaluation of Hydrogen Storage Capacity in Pure Carbon Nanostructures. *J. Chem. Phys.* **2003**, *119*, 2376–2385.
- (5) Targets for Onboard Hydrogen Storage Systems for Light-duty Vehicles (US DOE 2009), http://www.eere.energy.gov/hydrogenandfuelcells/storage/pdfs/targets_onboard_hydro_storage_explanation.pdf.
- (6) Alonso, J. A.; Cabria, I.; López, M. J. Simulation of Hydrogen Storage in Porous Carbons. *J. Mater. Res.* **2013**, *28*, 589–604.
- (7) López, M. J.; Cabria, I.; Alonso, J. A. Simulated Porosity and Electronic Structure of Nanoporous Carbons. *J. Chem. Phys.* **2011**, *135*, 104706.
- (8) Chen, P.; Wu, X.; Lin, J.; Tan, K. L. High H₂ Uptake by Alkali-Doped Carbon Nanotubes Under Ambient Pressure and Moderate Temperatures. *Science* **1999**, *285*, 91–93.
- (9) Yang, R. T. Hydrogen Storage by Alkali-Doped Carbon Nanotubes-Revisited. *Carbon* **2000**, *38*, 623–626.
- (10) Bath, V. V.; Contescu, C. I.; Gallego, N. C.; Baker, F. S. Atypical Hydrogen Uptake on Chemically-Activated, Ultramicroporous Carbon. *Carbon* **2010**, *48*, 1331–1340.

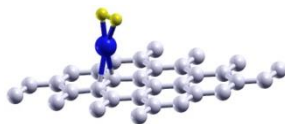
- (11) Cabria, I.; López, M. J.; Alonso, J. A. Enhancement of Hydrogen Physisorption on Graphene and Carbon Nanotubes by Li Doping. *J. Chem. Phys.* **2005**, *123*, 204721.
- (12) Cabria, I.; López, M. J.; Alonso, J. A. Hydrogen Storage in Pure and Li-doped Carbon Nanopores: Combined Effects of Concavity and Doping. *J. Chem. Phys.* **2008**, *128*, 144704.
- (13) Kiran, B.; Kandalam, A. K.; Jena, P. Hydrogen Storage and the 18-Electron Rule. *J. Chem. Phys.* **2006**, *124*, 224703.
- (14) Zhao, Y.; Kim, Y.-H.; Dillon, A. C.; Heben, M. J.; Zhang, S. B. Hydrogen Storage on Novel Organometallic Buckyballs. *Phys. Rev. Lett.* **2005**, *94*, 155504.
- (15) Durgun, E.; Jang, Y. R.; Ciraci, S. Hydrogen Storage Capacity of Ti-Doped Boron-Nitride and B/Be-Substituted Carbon Nanotubes. *Phys. Rev. B* **2007**, *76*, 073413.
- (16) Yildirim, T.; Ciraci, S. Titanium-Decorated Carbon Nanotubes as a Potential High-Capacity Hydrogen Storage Medium. *Phys. Rev. Lett.* **2005**, *94*, 175501.
- (17) Kubas, G. J. Metal-Dihydrogen and σ -Bond Coordination: The Consummate Extension of the Dewar-Chatt Duncanson Model for Metal-Olefin π Bonding. *J. Organomet. Chem.* **2001**, *635*, 37–68.
- (18) Niu, J.; Rao, B. K.; Jena, P. Binding of Hydrogen Molecules by a Transition-Metal Ion. *Phys. Rev. Lett.* **1992**, *68*, 2277–2280.
- (19) Cabria, I.; López, M. J.; Alonso, J. A. Theoretical Study of the Transition from Planar to Three-Dimensional Structures of Palladium Clusters Supported on Graphene. *Phys. Rev. B* **2010**, *81*, 035403.
- (20) Sun, Q.; Wang, Q.; Jena, P.; Kawazoe, Y. Clustering of Ti on a C₆₀ Surface and its Effect on Hydrogen Storage. *J. Am. Chem. Soc.* **2005**, *127*, 14582.

- (21) Krasnov, P. O.; Ding, F.; Singh, A. K.; Yakobson, B. I. Clustering of Sc on SWNT and Reduction of Hydrogen Uptake: Ab-initio All Electron Calculations. *J. Phys. Chem. C* **2007**, *111*, 17977–17980.
- (22) Kim, G.; Jhi, S. H.; Lim, S.; Park, N. Effect of Vacancy Defects in Graphene on Metal Anchoring and Hydrogen Adsorption. *Appl. Phys. Lett.* **2009**, *94*, 173102.
- (23) Lim, D. H.; Negreira, A. S.; Wilcox, J. DFT Studies on the Interaction of Defective Graphene-Supported Fe and Al Nanoparticles. *J. Phys. Chem. C* **2011**, *115*, 8961–8970.
- (24) Fair, K. M.; Cui, X. Y.; Li, L.; Shieh, C. C.; Zheng, R. K.; Liu, Z. W.; Delley, B.; Ford, M. J.; Ringer, S. P.; Stampfl, C. Hydrogen Adsorption Capacity of Adatoms on Double Carbon Vacancies of Graphene: A Trend Study from First Principles. *Phys. Rev. B* **2013**, *87*, 014102.
- (25) Vanderbilt, D. Soft Self-Consistent Pseudopotentials in a Generalized Eigenvalue Formalism. *Phys. Rev. B* **1990**, *41*, R7892.
- (26) dacapo, See <https://wiki.fysik.dtu.dk/dacapo> for a description of the total energy code, based on the density functional theory. 2009.
- (27) Perdew, J. P.; Wang, Y. Accurate and Simple Analytic Representation of the Electron-Gas Correlation Energy. *Phys. Rev. B* **1992**, *45*, 13244.
- (28) Monkhorst, H.; Pack, J. Special Points for Brillouin-Zone Integration. *Phys. Rev. B* **1976**, *13*, 5188–5192.
- (29) Cabria, I.; López, M. J.; Fraile, S.; Alonso, J. A. Adsorption and Dissociation of Molecular Hydrogen on Palladium Clusters Supported on Graphene. *J. Phys. Chem. C* **2012**, *116*, 21179–21189.

- (30) Contescu, C. I.; van Benthem, K.; Li, S.; Bonifacio, C. S.; Pennycook, S. J.; Jena, P.; Gallego, N. C. Single Pd Atoms in Activated Carbon Fibers and their Contribution to Hydrogen Storage. *Carbon* **2011**, *49*, 4050–4058.
- (31) Thrower, P. A.; Mayer, R. M. Point Defects and Self-Diffusion in Graphite. *Phys. Stat. Sol. (a)* **1978**, *47*, 11–37.
- (32) Ma, Y.; Lehtinen, P. O.; Foster, A. S.; Nieminen, R. M. Magnetic Properties of Vacancies in Graphene and Single-Walled Carbon Nanotubes. *New J. Phys.* **2004**, *6*, 68.
- (33) Singh, R.; Kroll, P. Magnetism in Graphene due to Single-Atom Defects: Dependence on the Concentration and Packing Geometry of Defects. *J. Phys.-Condes. Matter* **2009**, *21*, 196002.
- (34) Bhatia, S. K.; Myers, A. L. Optimum Conditions for Adsorptive Storage. *Langmuir* **2006**, *22*, 1688–1670.

Figure 8: Table of Contents- graphics

H₂@Pd@pristine graphene



H₂@Pd@graphene vacancy

